Articles

Highly Efficient Multi-Functional Material for Organic Light-Emitting Diodes; Hole Transporting Material, Blue and White Light Emitter[†]

Myoung Ki Kim, Jongchul Kwon, Jung-Pyo Hong, Seonghoon Lee, and Jong-In Hong[*]

Department of Chemistry, College of Natural Sciences, Seoul National University, Seoul 151-747, Korea
[*]E-mail: jihong@snu.ac.kr

We have demonstrated that **TPyPA** can be used as an efficient multi-functional material for OLEDs; hole transporting material (HTL), blue and white-light emitter. The device based on **TPyPA** as the HTL exhibited an external quantum efficiency of 1.7% and a luminance efficiency of 4.2 cd/A; these values are 40% higher than the external quantum efficiency and luminance efficiency of the NPD-based reference device. The device based on **TPyPA** as a blue-light emitter exhibited an external quantum efficiency of 4.2% and a luminance efficiency of 5.3 cdA^{-1} with CIE coordinates at (0.16, 0.14), the device based on **TPyPA** as a white-light emitter exhibited an external quantum efficiency of 3.2% and a luminance efficiency of 7.7 cdA^{-1} with CIE coordinates at (0.33, 0.39). Also, **TPyPA**-based organic solar cell (OSC) exhibited a maximum power conversion efficiency of 0.35%. **TPyPA**-based organic thin-film transistors (OTFTs) exhibited highly efficient field-effect mobility (μ_{FET}) of 1.7×10^{-4} cm^2 V^{-1} s^{-1}, a threshold voltage (V_{th}) of −15.9 V, and an on/off current ratio of 8.6×10^3.

Key Words : OLEDs, Hole transport material, Blue emitter, White OLEDs, Multi-functional material

Introduction

Pyrene has been used as a signaling unit for fluorescent probes, owing to its high photoluminescence efficiency[1] and excimer-formation property.[2] Recently, pyrene has been used in various fields involving photo-catalysts,[3] semiconductors,[4] charge-transfer,[5] crystals,[6] carbon nanotubes,[7] DNA probes,[8] and dendrimers.[9] In particular, blue fluorescent emitters based on pyrene units have attracted considerable attention for organic light-emitting diodes (OLEDs), owing to the advantages of pyrene.[10,11] The photoluminescence quantum yield, carrier mobility, and hole-injection ability of emitters that consist of pyrene units are higher when compared to those of emitters that consist of oligofluorenes or polyfluorenes.[11a]

Several groups have reported a series of pyrene-based materials that can act as blue-light emitters and other functional materials.[11] Since pyrene can act as an emitter as well as a hole-transporting layer (HTL) and an electron-transporting layer (ETL), (both of which are extremely important for OLEDs,) simple electroluminescent (EL) devices based on pyrene have been fabricated.[12] Similarly, tris(8-hydroxyquinoline)aluminum(III) (Alq$_3$), which acts as an ETL material as well as an emitting material, is also used for the fabrication of simple EL devices.[12a] Huang *et al*. have reported that blue- and white-light emitting OLEDs can be

fabricated using pyrene derivatives as emitters; these OLEDs exhibited a luminance efficiency of 1.30 cdA^{-1} with CIE coordinates at (0.16, 0.10) and 1.84 cdA^{-1} with CIE coordinates at (0.29, 0.38), respectively.[11a] Wang *et al*. have reported blue-light emitting and hole-transporting bi-functional materials; these pyrene derivatives exhibit a luminance efficiency of 0.97 cdA^{-1} with wavelength at 440 nm when used as a blue emitter and a luminance efficiency of 0.40 cdA^{-1} with wavelength at 453 nm when used as a hole-transporting material.[11b] The blue- and white-light emitting OLEDs that use pyrene derivatives as emitters do not exhibit high luminance efficiency or excellent CIE coordinates. Although these materials did not exhibit a high OLEDs performance, it is notable achievement that pyrene derivatives have been used as bi-functional materials for OLED materials.

Several groups have reported bi-functional materials that can act either as OLED and field-effect transistor materials using triphenylamine-oligothiophene conjugated systems or as OLED and organic solar cell (OSC) materials using multi-triarylamine substituted carbazole based dendrimers with an oligothiophene core, Berggren *et al*. introduced multifunctional materials which can be used for OSC, OLEDs, OTFTs due to their the low cost, simple device fabrication, flexible organic electronic devices in manufacturing process of organic electronic devices.[13]

In this paper, we report that high efficiency optoelectronics devices can be realized using 4,4',4"-trispyrenylphenylamine (**TPyPA**).[13c] We demonstrate that **TPyPA** can be used as a hole-transporting material, a blue-light emitting material,

---

[†]This paper is dedicated to Professor Eun Lee on the occasion of his honourable retirement.

and a white-light emitting material for OLEDs. Moreover, **TPyPA** can also be used as a donor material for OSCs and as an active material for organic thin-film transistors (OTFTs). OLED devices based on **TPyPA** as the HTL exhibit an external quantum efficiency of 1.7% and a luminance efficiency of 4.2 cdA^{-1}; these values are 40% higher compared to 4,4'-bis[*N*-(naphthyl-*N*-phenylamino)biphenyl (α-NPD), which is a widely used HTL, based reference device (1.2% and 3.0 cdA^{-1}, respectively). The OLED devices based on **TPyPA** as a blue-light emitter exhibit an external quantum efficiency of 4.2% and a luminance efficiency of 5.3 cdA^{-1} with CIE coordinates of (0.16, 0.14), while the OLED device using **TPyPA** as a white-light emitter exhibit an external quantum efficiency of 3.2% and a luminance efficiency of 7.7 cdA^{-1} with CIE coordinates of (0.33, 0.39). To our surprise, among the multi-functional materials reported in the literature, **TPyPA** is a material with one of the highest efficiencies as a blue- and white-light emitter for OLEDs.[11,13,14] **TPyPA**-based OSCs exhibit a maximum power conversion efficiency of 0.35%. The **TPyPA**-based OTFTs exhibit a field-effect mobility (μ_{FET}) of 1.7×10^{-4} cm^2 V^{-1} s^{-1}, a threshold voltage (V_{th}) of -15.9 V, and an on/off current ratio of 8.6×10^3.

Experimental Section

Materials and Instrument. The organic materials such as C$_{60}$, CuPc, NPD, and CBP were purchased from Aldrich, Lumtree, and Gracel. UV-vis spectra were recorded on a Beckman DU 650 spectrophotometer, and fluorescence spectra were recorded on a Jasco FP-7500 spectrophotometer. CV measurement was performed using a CH Instruments Model 660 Electrochemical Analyzer (CH Instruments, Inc., Texas). Atomic force microscopy (AFM) experiments were performed using an Asylum MFP-3D instrument in AC mode with Si$_3$N$_4$ cantilevers, and XRD analyses were carried out with a Rigaku ($\lambda = 1.5418$ Å, 298 K) X-ray diffractometer. The decomposition temperatures (T$_d$) were obtained using a thermal gravimetric analyzer from Rheometric Scientific.

Synthesis. 4,4',4"-Trispyrenylphenylamine (**TPyPA**): A mixture of tris(4-bromophenyl)amine (1.23 g, 2.57 mmol), 1-pyreneboronic acid (1.90 g, 7.72 mmol), 2 M potassium carbonate solution (20 mL), and palladium tetrakis (triphenylphosphine) (148 mg, 0.103 mmol) in THF/H$_2$O was heated at 80 ^{o}C for seven days. After cooling to room temperature, all the volatiles were evaporated in vacuum, and the reaction mixture was extracted using dichloromethane. The organic phase was washed with water and dried over MgSO$_4$. The solvent was evaporated in order to obtain the product, which was applied to column chromatography on silica gel using ethyl acetate and hexane as the eluents (1:20) and recrystallized from dichloromethane and hexane in order to obtain a solid product (Yield: 1.18 g, 54%). ^{1}H NMR (300 MHz, CDCl$_3$): δ 8.41 (d, 9 Hz, 3H), 8.27 (d, 9 Hz, 3H), 8.23 (d, 9 Hz, 6H), 8.18 (d, 12 Hz, 3H), 8.13 (d, 3 Hz, 6H), 8.10 (d, 3 Hz, 3H), 8.04 (d, 15 Hz, 3H), 7.70 (d, 9 Hz, 6H). 7.59 (d, 9 Hz, 6H). ^{13}C NMR (125 MHz, CDCl$_3$): δ 147.1, 137.6, 136.0, 131.8, 131.7, 131.2, 130.7, 128.7,

127.9, 127.6, 127.5, 126.2, 125.6, 125.4, 125.3, 125.2, 125.1, 125.0, 124.9, 124.4. Mass: calculated for C$_{66}$H$_{39}$N [M]$^+$ 846.3161, HR-Mass: 846.3167.

OLED Fabrication. A 10-nm-thick CuPc layer was used as the HIL and a 60-nm-thick layer of NPD was used as the HTL. A 30-nm-thick emitting layer (EML) was prepared by co-evaporating ADN as the host and 5, 50 wt % of TPyPA as the fluorescent dopant. Next, a 20-nm-thick layer of Balq, which was used as a hole-blocking layer (HBL) and ETL, was evaporated. Subsequently, LiF, which was used as an electron injection layer (EIL), was also evaporated. Finally, a 100-nm-thick layer of aluminum was deposited onto the LiF layer. A PR-650 source meter with a computer was used to operate the device.

OSC Fabrication. A 30-nm-thick layer of PEDOT:PSS was used as the HIL. Various films containing TPyPA layers of various thicknesses, varying from 10 nm to 30 nm, were prepared by the evaporation process. Subsequently, a 40-nm-thick layer of fullerene (C$_{60}$), used as an acceptor, was also evaporated onto the film. Next, a 5-nm-thick layer of BCP used as an EBL was evaporated. Finally, a 100-nm-thick layer of aluminum was evaporated onto the BCP layer. A current-voltage measurement of the devices was performed on a Keithley instrument. A xenon lamp coupled with AM 1.5 solar spectra was used as the light source. The light intensity at each wavelength was calibrated with a standard silicon solar cell as a reference.
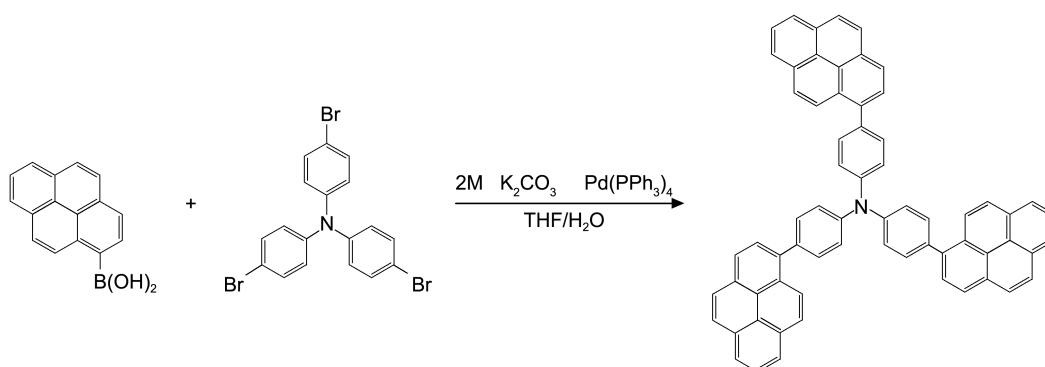
OTFT Fabrication. The TPyPA-based OTFTs were fabricated using top-contact geometry. We used a heavily doped Si wafer as the gate electrode and a non-pretreated or octadecyltrichlorosilane (OTS)-pretreated SiO$_2$ layer (thickness: approximately 300 nm) as the gate dielectric. Prior to deposition, the TPyPA starting material was purified by temperature gradient vacuum sublimation to improve the purity of the active layer. The TPyPA films (thickness: ca. 50 nm) were then grown by vacuum sublimation by using a homemade apparatus at a rate range of 0.4 to 0.8 Å/s under a working pressure of 2.0×10^{-6} to 2.5×10^{-6} torr. Gold source/drain electrodes were evaporated on top of the films through a shadow mask with a channel length (*L*) of 50 μm and a channel width (*W*) of 1000 μm. Electrical characterization of the transistors was performed in air at room temperature by using a Keithley 4200-SCS semiconductor analyzer. The field-effect mobility (μ) was calculated in the saturation region ($V_{DS} = -100$ V) from the plot of the square-root of the drain current *vs* V_{GS} using the following equation:

$$I_{DS} = \frac{WC_i}{2L}\mu(V_{GS} - V_T)^2$$

where I_{DS} is the source-drain saturation current, C_i (1.1×10^{-8} F) is the capacitance of the SiO$_2$ insulator, *W/L* is the ratio of the width to the channel length, and V_{GS} and V_T are the gate-source and threshold voltages, respectively.

Results and Discussion

TPyPA was synthesized by the Suzuki coupling between
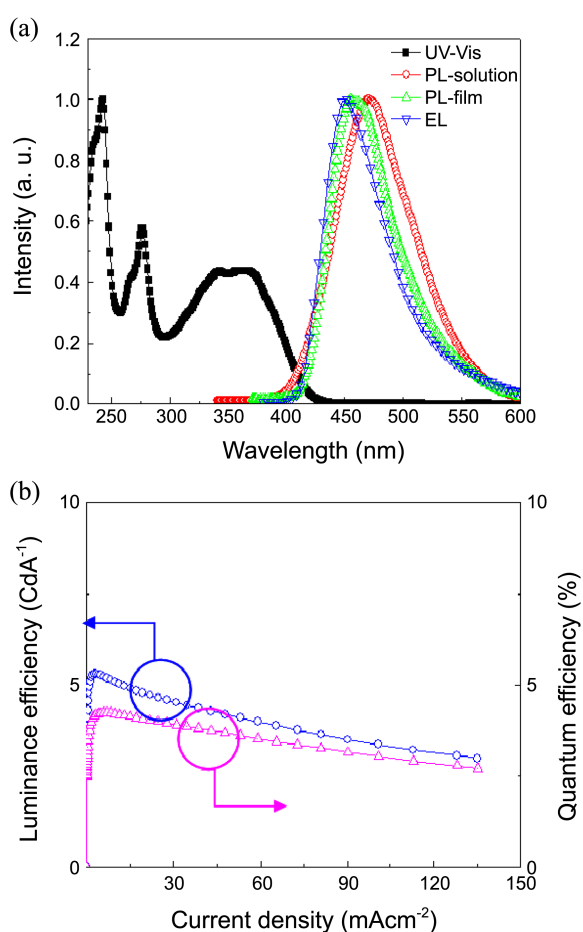
Scheme 1. The synthesis of TPyPA.

Figure 1. (a) UV-vis and PL spectra of TPyPA in 0.02 mM CH_2Cl_2 and PMMA film and EL spectra of device 1. (b) Luminance efficiency *vs* current density and quantum efficiency *vs* current density for the device using **TPyPA** as a blue emitter [device 1; ITO/CuPc (10 nm)/NPD (60 nm)/5% **TPyPA**:ADN (30 nm)/Balq (20 nm)/LiF (1 nm)/Al (100 nm)].

1-pyreneboronic acid and tris(4-bromophenyl)amine (Scheme 1). The UV spectra of **TPyPA** exhibited multiple absorption bands at 242, 276, 337, and 367 nm in CH_2Cl_2, and the PL spectra of **TPyPA** exhibited a blue emission at 470 nm in CH_2Cl_2 and a deep-blue emission at 452 nm in polymethylmethacrylate (PMMA) film (Figure 1(a)). Interestingly, the PL spectra of **TPyPA** in the PMMA film exhibited a blue

shift in comparison to the PL spectra of **TPyPA** in CH_2Cl_2; this phenomenon is rarely observed because of solvatochromic effect.[11b] Using anthracene as a standard, the PL quantum yield of **TPyPA** was estimated to be 0.38 (Table S1).[15] Thermal gravimetric analysis (TGA) data revealed that **TPyPA** has a good thermal stability (T_d = 572 °C and T_g = 142 °C). The T_g value of **TPyPA** was higher than that of NPD (T_g = 96 °C) (Figure S1). Further, we carried out a cyclic voltammetry (**CV**) measurement to study the electrochemical properties of **TPyPA**. The CV data showed the occurrence of a reversible oxidation process associated with the generation of a stable cation radical. However, the reduction potential of **TPyPA** was not observed in the CV measurement. The half-oxidation potential of **TPyPA** was observed at $E_{1/2}$ = 0.37 V after ferrocene/ferrocenium (Fc/Fc^+) correlation. From the above mentioned results and the cross-section wavelength between the absorption and emission spectra, the HOMO and LUMO energy values of **TPyPA** were calculated to be −5.60 eV and −2.60 eV, respectively (Table S1, Figure S2).

We examined the PL spectra of **TPyPA** in a solid film while increasing the doping ratio of **TPyPA** in 9,10-di(2-naphthyl)anthracene (ADN = host) in order to confirm the energy transfer between the host and **TPyPA** (the dopant). At **TPyPA** doping levels of (up to) 1% and 3%, the host spectra appeared at 370 nm and the **TPyPA** spectra appeared at around 450-465 nm. At **TPyPA** doping levels of up to 50% and 100%, the host spectra (at 370 nm) disappeared, and the **TPyPA** spectra and new spectra from the excimer of **TPyPA** appeared at around 560 nm. At **TPyPA** doping levels of up to 5% in the host, the PL spectra of the film exhibited a strong emission intensity originating only from **TPyPA**. Thus, it can be inferred that a doping ratio of 5% is suitable for blue-light emitting OLEDs, while doping ratios of 50% and 100% are suitable for white-light emitting OLEDs (Figure S3).

In order to investigate the multi-functional properties of TPyPA, we fabricated three types of OLEDs. First, we fabricated a blue-emitting OLED device using 9, 10-di(2-naphthyl)anthracene (ADN) as the host and **TPyPA** as the fluorescent dopant. The EL device was constructed via sequential vacuum deposition with the device structure of ITO/CuPc (10 nm)/NPD (60 nm)/5% **TPyPA**:ADN (30 nm) /Balq (20 nm)/LiF (1 nm)/Al (100 nm) (device 1). Copper

Table 1. Layer structures and EL performance data of the OLED devices

Device	Q.E. (%)[a]	P.E. (lm W^{-1})[b]	C.E. (cd A^{-1})[c]	EL (nm)	CIE
1	4.2	2.1	5.3	450	(0.16, 0.14)
2	2.9	3.5	5.7	475, 565	(0.33, 0.41)
3	3.2	5.8	7.7	475, 565, 615	(0.33, 0.39)
4	1.7.	2.9	4.2	545	(0.38, 0.53)

[a]Maximum quantum efficiency. [b]Maximum power efficiency. [c]Maximum luminance efficiency Device 1; ITO/CuPc (10 nm)/NPD (60 nm)/5% TPyPA : ADN (30 nm)/Balq (20 nm)/LiF (1 nm)/Al (100 nm). Device 2; ITO/CuPc (10 nm)/NPD (60 nm)/50% TPyPA : ADN (30 nm)/Balq (20 nm)/LiF (1 nm)/Al (100 nm). Device 3; ITO/CuPc (10 nm)/NPD (60 nm)/50% TPyPA : ADN (30 nm)/ Ir(piq)$_2$ acac 10% : Balq (5 nm)/Balq (15 nm)/LiF (1 nm)/ Al (100 nm). Device 4; ITO/TPPA (70 nm)/Alq$_3$ (60 nm)/LiF (1 nm)/Al (100 nm).

phthalocyanine (CuPc) was used as the hole-injection layer (HIL); NPD, as the HTL; and 4-biphenyloxolatoaluminium(III) bis(2-methyl-8-quinolinato)-4-phenylphenolate (Balq), as the ETL. The OLED device using a ratio of 5:95 of **TPyPA** and ADN demonstrated a stable deep blue emission with CIE coordinates of (0.16, 0.14), a high luminance efficiency of 5.3 cdA^{-1}, and an external quantum efficiency of 4.2% with the maximum EL peak at 450 nm (Figure 1, Table 1). To the best of our knowledge, this blue-emitting device exhibited one of the highest luminance efficiencies among the pyrene-based deep-blue emitters ever reported.[10-12]

Next, the white-emitting device with the device structure ITO/CuPc (10 nm)/NPD (60 nm)/50% **TPyPA**:ADN (30 nm)/Balq (20 nm)/LiF (1 nm)/Al (100 nm) (device 2) was fabricated. The OLED device using 1:1 of **TPyPA** and ADN exhibited a white emission with CIE coordinates of (0.33, 0.41) because of emission from the excimer or exciplex,[13c,16b] a luminance efficiency of 5.7 cdA^{-1}, and an external quantum efficiency of 2.9% with EL peaks at 475 nm and 565 nm (Figure 2). The OLED device using **TPyPA** as a white-light emitter exhibited excellent CIE coordinates and had a high efficiency, considering that only a single emitter was used.[16]

To improve the CIE coordinates to the National Television System Committee (NTSC) standard for white emission (0.33, 0.33), we fabricated a new OLED device using bis(1-phenyl-isoqunolinato-N,C2')iridium(acetylacetonate) [Ir(piq)$_2$acac] as a red phosphorescent material. The EL device was constructed with the device structure ITO/CuPc (10 nm)/NPD (60 nm)/50% **TPyPA**:ADN (30 nm)/10% Ir(piq)$_2$acac:Balq (5 nm)/Balq (15 nm)/LiF (1 nm)/Al (100 nm) (device 3). The device exhibited a white emission with CIE coordinates at (0.33, 0.39), a luminance efficiency of 7.7 cdA^{-1}, and an external quantum efficiency of 3.2% with EL peaks at 470 nm, 565 nm, and 615 nm (Figure 2). The CIE coordinates were close to the NTSC standard for white emission (0.33, 0.33), and the efficiency of the device was increased by using red phosphorescent materials, owing to the participation of previously wasted triplet excitons in the emission process.[18a] This result demonstrated that when compared to other OLED devices, the **TPyPA**-based OLED device can achieve a white emission with excellent efficiency by incorporating a simple FP (fluorescent/phosphorescent) structure.[18]

In order to confirm the hole-transporting nature of TPyPA, we fabricated an OLED device using **TPyPA** as the HTL material. The EL device was constructed with the device structure ITO/**TPyPA** (70 nm)/Alq$_3$ (60 nm) /LiF (1 nm)/Al
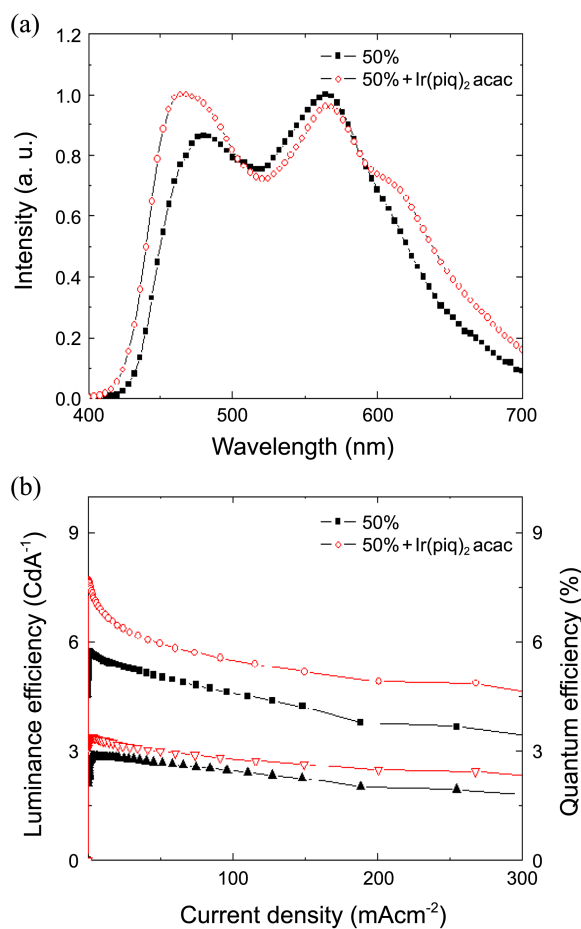

Figure 2. Device performance of device 2-ITO/CuPc (10 nm)/NPD (60 nm)/50% **TPyPA**:ADN (30 nm)/Balq (20 nm)/LiF (1 nm)/Al (100 nm)- and device 3-ITO/CuPc (10 nm)/NPD (60 nm)/50% TPyPA:ADN(30 nm)/10% Ir(piq)$_2$acac:Balq (5 nm)/Balq (15 nm)/ LiF (1 nm)/Al (100 nm); (a) EL spectra; (b) luminance efficiency *vs* current density and quantum efficiency *vs* current density.

(100 nm) (device 4); Alq$_3$ was used as an electron-transporting material and emitting material. This device exhibited a green emission from Alq$_3$ with CIE coordinates at (0.38, 0.53) and a luminance efficiency of 4.2 cdA^{-1} (Figure 3), which is 40% higher than that of the NPD-based reference device (3.0 cdA^{-1}). In particular, the device using **TPyPA** as the HTL exhibited a higher turn-on voltage than the NPD-based device due to the hole injection barrier of **TPyPA** being higher than that of NPD. However, the luminance and efficiency of the **TPyPA**-based devices were higher than
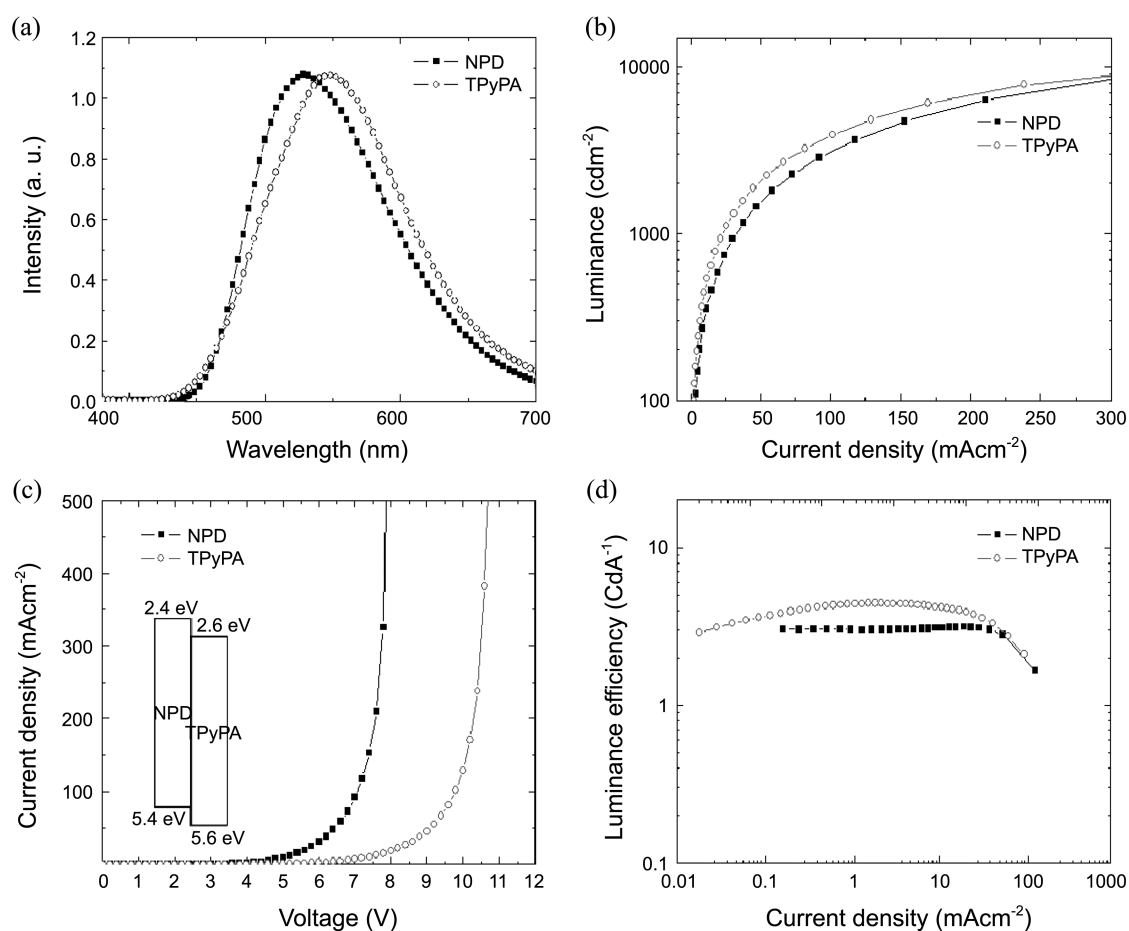
(a)

(b)

(c)

(d)

Figure 3. Device performance of NPD and TPyPA as the HTL: (a) EL spectra; (b) current density *vs* luminance; (c) voltage *vs* current density (inset: HOMO and LUMO energy levels of NPD and TPyPA); (d) current density *vs* current efficiency.

those of the NPD-based devices. This is because of improved hole mobility, which improves the charge balance of holes and electrons in Alq3.[19] The hole mobility of **TPyPA** was 1.7×10^{-4} cm^2 V^{-1} s^{-1} and that of NPD was 1.2×10^{-5} cm^2 V^{-1} s^{-1} (Table S2); the increased hole mobility resulted from the introduction of the triphenylamine group into the pyrene molecule.[11b,16b] As a result, to the best of our knowledge, **TPyPA** exhibits one of the best efficiencies as a blue- and white-light emitter and as a HTL material for OLEDs among pyrene-based materials,[11,12] and multi-functional materials reported in the literature.[11,13,14]

Moreover, we used a **TPyPA** for OSC and OTFTs, since introducing multifunctional materials which can be used for OSC, OLEDs, OTFTs have some merits; the low cost, simple device fabrication, flexible organic electronic devices in manufacturing process of organic electronic devices.[13d] First, we investigated the OSC properties using **TPyPA** as a donor. The OSC devices were constructed with the device structure ITO/PEDOT:PSS (30 nm)/**TPyPA**(*x* nm)/C$_{60}$ (40 nm)/BCP (5 nm)/Al (100 nm); poly(3,4-ethylenedioxythiophene)poly (styrenesulfonate) (PEDOT:PSS) was used as the HIL. Films containing **TPyPA** layers of various thicknesses, varying from 10 nm to 30 nm, were prepared by the evaporation process. Subsequently, a 40-nm-thick layer of fullerene (C$_{60}$) was

evaporated onto the film as an acceptor, and a 5-nm-thick layer of BCP (2,9-dimethyl-4,7-diphenyl-1,10-phenanthroline) was evaporated as an exciton-blocking layer (EBL). Finally, a 100-nm-thick layer of aluminum was evaporated onto the BCP layer. A current-voltage measurement of the devices was performed on a Keithley instrument. A xenon lamp
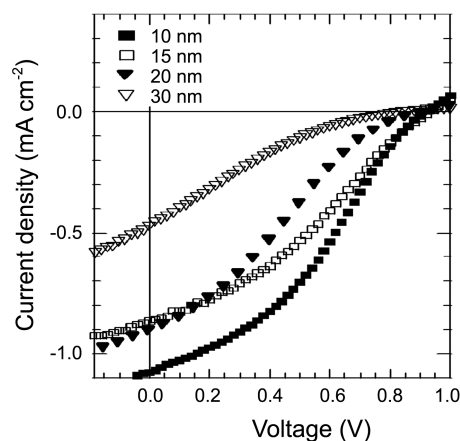
Figure 4. I-V characteristics of ITO/PEDOT (30 nm)/**TPyPA** (*x* nm)/C$_{60}$ (40 nm)/BCP (5 nm)/Al (100 nm) devices under simulated AM 1.5 solar irradiation at 100 mW/Cm^2.

Table 2. Heterojunction device data for various film thicknesses of TPyPA and C_{60} under simulated AM 1.5 solar irradiation at 100 mWcm^{-2}

Thickness of TPyPA	V_{OC} (V)[a]	I_{SC} (mACm^{-2})[b]	FF (%)[c]	PCE (%)[d]
10 nm	0.91	1.0	35	0.35
15 nm	0.93	0.86	33	0.26
20 nm	0.92	0.90	25	0.21
30 nm	0.87	0.47	17	0.07

[a]open circuit voltage. [b]short circuit current. [c]fill factor. [d]power conversion efficiency

coupled with AM 1.5 solar spectra was used as the light source. The light intensity at each wavelength was calibrated with a standard silicon solar cell as reference. The device with a 10-nm-thick layer of **TPyPA** exhibited a maximum power conversion efficiency (PCE) of 0.35% and a short-circuit current (I_{sc}) of 1.0 m A cm^{-2}. Those devices in which the thickness of the **TPyPA** layer was greater than 15 nm exhibited a short-circuit current of 0.86 mA cm^{-2} and a power conversion efficiency of 0.26%. In particular, the 20-nm-thick **TPyPA**-based device exhibited a slightly lower power conversion efficiency of 0.21% and a short-circuit

(a)

(b)

Figure 5. (a) output of the OTFTs using **TPyPA** (b) transfer characteristics of the OTFTs using **TPyPA** deposited on OTS treated SiO$_2$ at T$_{sub}$ = 75 °C.

current of 0.90 mA cm^{-2}. However, as the thickness of the **TPyPA** layer was further increased to 30 nm, the device exhibited a significantly lower short-circuit current of 0.47 mA cm^{-2} and a power conversion efficiency of 0.07%; this was because the excitons in films with thick **TPyPA** layers were not able to efficiently separate into holes and electrons. Due to the narrow absorption range of **TPyPA**, **TPyPA**-based devices did not exhibit power conversion efficiency greater than 0.35% (Figure 4). The overall device performance data of the devices based on **TPyPA** and C$_{60}$ are summarized in Table 2.

Second, we investigated OTFT properties using **TPyPA** as the active layer. The transistors based on TPyPA were fabricated using the top contact geometry. Figure 5 shows the output and transfer characteristics of top-contact OTFTs in which **TPyPA** was deposited at a substrate temperature (T_{sub}) of 75 °C on octadecyltrichlorosilane (OTS)-treated SiO$_2$. From electrical transfer characteristics, we obtained the parameters of the OTFTs, such as field-effect mobility, on/off current ratio, and threshold voltage. The **TPyPA**-based OTFTs exhibited a field-effect mobility (μ_{FET}) of 1.7×10^{-4} cm^2 V^{-1}s^{-1}, a threshold voltage (V_{th}) of -15.9 V, and an on/off current ratio of 8.6×10^3 at 75 °C. The electrical properties of the **TPyPA**-based OTFTs fabricated under various conditions are summarized in Table S2. The field-effect mobilities of **TPyPA**-based OTFTs are similar to those of the OTFTs derived from other triphenylamine (TPA) derivatives. The moderate field-effect motilities of the OTFT devices derived from TPA derivatives and **TPyPA** are presumably due to the difficulty in maintaining TPA derivatives and **TPyPA** in perpendicular geometry with respect to the substrate.

Conclusion

In summary, we have demonstrated that **TPyPA** can be used as an efficient multi-functional material for OLEDs; hole transporting material (HTL), blue and white-light emitter. The OLED device based on **TPyPA** as a HTL exhibited an external quantum efficiency of 1.7% and a luminance efficiency of 4.2 cdA^{-1}; these values were 40% higher than the external quantum efficiency and luminance efficiency of the NPD-based reference device. The device based on **TPyPA** as a blue-light emitter exhibited an external quantum efficiency of 4.2% and a luminance efficiency of 5.3 cdA^{-1} with CIE coordinates at (0.16, 0.14), and the device based on **TPyPA** as a white-light emitter exhibited an external quantum efficiency of 3.4% and a luminance efficiency of 7.7 cdA^{-1} with CIE coordinates at (0.33, 0.39). Moreover, the **TPyPA**-based OSC exhibited a maximum power conversion efficiency of 0.35%. The **TPyPA**-based OTFTs exhibited moderate field-effect mobility (μ_{FET}) of 1.7×10^{-4} cm^2 V^{-1} s^{-1}, a threshold voltage (V_{th}) of -15.9 V, and an on/off current ratio of 8.6×10^3. Consequently, **TPyPA** was found to be an efficient multi-functional material that can be used as a blue- and white-light emitter and a donor material in OSCs as well as a charge transport channel in OTFTs.
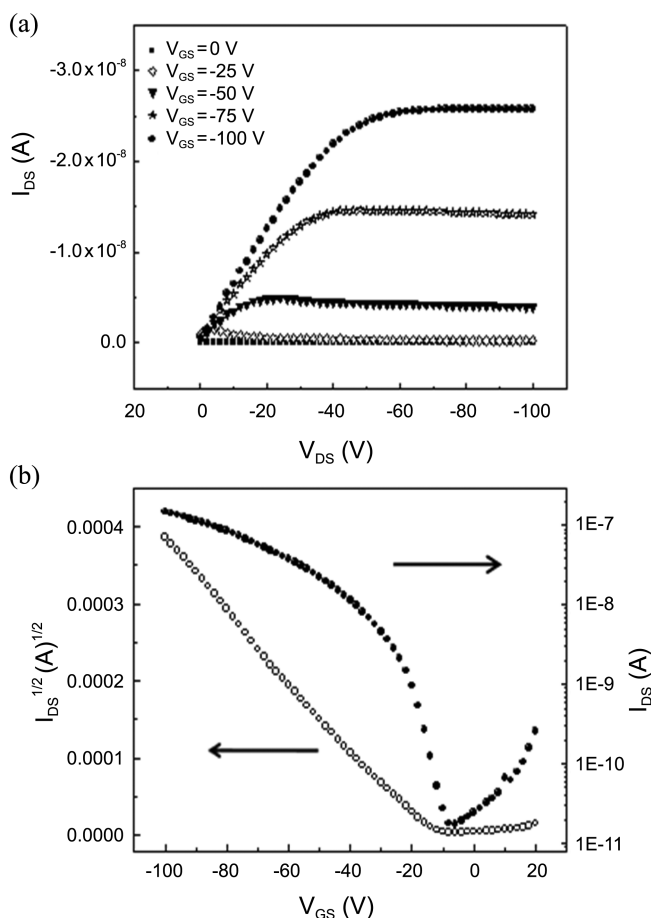
References

1. Bevilacqua, P. C.; Kierzek, R.; Johnson, K. A.; Turner, D. H. *Science* **1992**, *258*, 1355.
2. (a) Winnik, F. M. *Chem. Rev.* **1993**, *93*, 587. (b) Yang, R.-H.; Lee, W.-H.; Chan, A. W.; Xia, M. P.-F.; Zhang, H.-K.; Li, K. A. *J. Am. Chem. Soc.* **2003**, *125*, 2884. (c) Langenegger, S. M.; Häner, R. *Chem. Commun.* **2004**, *24*, 2792.
3. Cuquerella, M. C.; Amrani, S. E.; Miranda, M. A.; Përez-Prieto, J. *J. Org. Chem.* **2009**, *74*, 3232.
4. Lucas, L. A.; Longchamp, D. M. D.; Richter, L. J.; Kline, R. J.; Fischer, D. A.; Kaafarani, B. R.; Jabbour, G. E. *Chem. Mater.* **2008**, *20*, 5743.
5. Altamirano, M. S.; Bohorquez, M. V.; Previtali, C. M.; Chesta, C. A. *J. Phys. Chem. A* **2008**, *112*, 589.
6. Sun, B.; Dreger, Z. A.; Gupta, Y. M. *J. Phys. Chem. A* **2008**, *112*, 10546.
7. Yang, Q.; Shuai, L.; Zhou, J.; Lu, F.; Pan, X. *J. Phys. Chem. B* **2008**, *112*, 12934.
8. Honcharenko, D.; Zhou, C.; Chattopadhyaya, J. *J. Org. Chem.* **2008**, *73*, 2829.
9. Kannaiyan, D.; Imae, T. *J. Phys. Chem. B* **2008**, *112*, 12934.
10. (a) Wu, K.-C.; Ku, P.-J.; Lin, C.-S.; Shih, H.-T.; Wu, F.-I.; Huang, M.-J.; Lin, J.-J.; Chen, I.-C.; Cheng, C.-H. *Adv. Funct. Mater.* **2008**, *18*, 67. (b) Tao, S.; Z. Y.; Lee, C.-S.; Lee, S.-T.; Huang, D.; Zhang, X. *J. Phys. Chem. C* **2008**, *112*, 14603. (c) Tang, C.; Liu, F.; Xia, Y.-J.; Xie, L.-H.; Wei, A.; Li, S.-B.; Fanab, Q.-L.; Huang, W. *J. Mater. Chem.* **2006**, *16*, 4. (d) Mikroyannidis, J. A.; Fenenko, L.; Adachi, C. *J. Phys. Chem. B* **2006**, *110*, 20317. (e) Peng, Z.; Tao, S.; Zhang, X.; Tang, J.; Lee, C. S.; Lee, S.-T. *J. Phys. Chem. C* **2008**, *112*, 2165.
11. (a) Liu, F.; Tang, C.; Chen, Q.-Q.; Shi, F.-F.; Wu, H.-B.; Xie, L.-H.; Peng, B.; Cao, Y.; Huang, W. *J. Phys. Chem. C* **2009**, *113*, 4641. (b) Jia, W.-L.; Cormick, T. M.; Liu, Q.-D.; Fukutani, H.; Motala, M.; Wang, R.-Y.; Tao, Y.; Wang, S. *J. Mater. Chem.* **2004**, *14*, 334.
12. (a) Shirota, Y.; *J. Mater. Chem.* **2000**, *10*, 1. (b) Jia, W. L.; Bai, D. R.; McCormick, T.; Liu, Q. D.; Motala, M.; Wang, R. Y.; Seward, C.; Tao. Y.; Wang, S. *Chem. Eur. J.* **2004**, *4*, 994.
13. (a) Cravino, A.; Roquet, S.; Alévêque, O.; Leriche, P.; Frére, P. *J. Chem. Mater.* **2006**, *18*, 2584. (b) Lu, J.; Xia, P. F.; Lo, P. K.; Tao, Y.; Wong, M. S. *Chem. Mater.* **2006**, *18*, 6194. (c) Tong, Q.-X.; Lai, S.-L.; Chan, M.-Y.; Tang, J.-X.; Kwon, H.-L.; Lee, C.-S.; Lee, S.-T. *Appl. Phys. Lett.* **2007**, *91*, 023503. (d) Berggren, M.; Nilsson, D.; Robinson, N. D. *Nature Mater.* **2007**, *6*, 4.
14. (a) Shirota, Y.; Kinoshita, M.; Noda, T.; Okumoto, K.; Ohara, T. *J. Am. Chem. Soc.* **2000**, *122*, 11. (b) Kinoshita, M.; Kita, H.; Shirota, Y. *Adv. Funct. Mater.* **2002**, *12*, 780. (c) Doi, H.; Kinoshita, M.; Okumoto, K.; Shirota, Y. *Chem. Mater.* **2003**, *15*, 1080.
15. Dawson, W. R.; Windsor, M. W. *J. Phys. Chem.* **1968**, *72*, 3255.
16. (a) Fadhel, O.; Gras, M.; Lemaitre, N.; Deborde, V.; Hissler, M.; Geffroy, B.; Rèau, R. *Adv. Mater.* **2009**, *21*, 1261. (b) Tao, S.; Zhou, Y.; Lee, C.-S.; Lee, S.-T.; Huangc, D.; Zhang, X. *J. Mater. Chem.* **2008**, *18*, 3981. (c) Liu, Y.; Nishiura, M.; Wang, Y.; Hou, Z. *J. Am. Chem. Soc.* **2006**, *128*, 5592.
17. Li, C.-L.; Su, Y.-J.; Tao, Y.-T.; Chou, P.-T.; Chien, C.-H.; Cheng, C.-C.; Liu, R. -S. *Adv. Funct. Mater.* **2005**, *15*, 387.
18. (a) Sun, Y.; Giebink, N. C.; Kanno, H.; Ma, B.; Thompson, M. E.; Forrest, S. R. *Nature* **2006**, *440*, 908. (b) Chen, P.; Xue, Q.; Xie, W.; Duan, Y.; Xie, G.; Zhao, Y.; Hou, J.; Liu, S.; Zhang, L.; Li, B. *Appl. Phys. Lett.* **2008**, *93*, 153508.
19. (a) Tao, S.; Lee, C. S.; Lee, S. T.; Zhang, X. *Appl. Phys. Lett.* **2007**, *91*, 013507. (b) Su, S. J.; Sasabe, H.; Takeda, T.; Kido, J. *Chem. Mater.* **2008**, *20*, 1691.